RESEARCH ARTICLE

Replication stress and FOXM1 drive radiation induced genomic instability and cell transformation

Zhentian Li[1], David S. Yu[1], Paul W. Doetsch[2], Erica Werner[3]*

1 Department of Radiation Oncology, Winship Cancer Institute, Emory University School of Medicine, Atlanta, Georgia, United States of America, **2** Laboratory of Genomic Integrity and Structural Biology, NIH, National Institute of Environmental Health Sciences, Research Triangle Park, North Carolina, United States of America, **3** Department of Cell Biology, Emory University School of Medicine, Atlanta, Georgia, United States of America

* ewerner@emory.edu

Abstract

In contrast to the vast majority of research that has focused on the immediate effects of ionizing radiation, this work concentrates on the molecular mechanism driving delayed effects that emerge in the progeny of the exposed cells. We employed functional protein arrays to identify molecular changes induced in a human bronchial epithelial cell line (HBEC3-KT) and osteosarcoma cell line (U2OS) and evaluated their impact on outcomes associated with radiation induced genomic instability (RIGI) at day 5 and 7 post-exposure to a 2Gy X-ray dose, which revealed replication stress in the context of increased FOXM1b expression. Irradiated cells had reduced DNA replication rate detected by the DNA fiber assay and increased DNA resection detected by RPA foci and phosphorylation. Irradiated cells increased utilization of homologous recombination-dependent repair detected by a gene conversion assay and DNA damage at mitosis reflected by RPA positive chromosomal bridges, micronuclei formation and 53BP1 positive bodies in G1, all known outcomes of replication stress. Interference with the function of FOXM1, a transcription factor widely expressed in cancer, employing an aptamer, decreased radiation-induced micronuclei formation and cell transformation while plasmid-driven overexpression of FOXM1b was sufficient to induce replication stress, micronuclei formation and cell transformation.

Introduction

Ionizing radiation is an effective and widely used tool for cancer treatment and control. Over 50% of cancer patients will be exposed to ionizing radiation at some point of their illness [1]. Therefore, because of radiation's wide use and improved cancer treatment outcomes, adverse effects such as malignancies secondary to radiation are becoming more concerning [2–4]. The mechanism for radiogenic cancers is unknown. All tissues are susceptible to develop radiation-induced tumors of low mutational load, without a unique signature resulting from a known mechanism [5, 6]. Ionizing radiation is considered a weak mutagen [2, 7], and

generates multiple types of lesions on DNA [8]. Among them, double strand breaks (DSB) are the most toxic, however can be readily repaired in normal cells or cause death or senescence in repair-impaired cells [9].

Ionizing radiation also generates responses in cells that have not been directly targeted, which include delayed genomic instability, bystander, clastogenic and transgenerational effects (reviewed in [10, 11]). The molecular mechanisms driving these responses and their impact on the overall effects of ionizing radiation remain poorly understood.

Among non-targeted effects, radiation induced genomic instability (RIGI) is a quite heterogeneous response defined by the increased rate of acquisition of *de novo* genomic alterations in the progeny of irradiated cells [12]. A diverse set of biological end points have been associated with genomic instability, including micronuclei formation, sister chromatid exchanges, chromosomal gaps, karyotypic abnormalities, microsatellite instability, homologous recombination, gene mutation and amplification, cellular transformation, clonal heterogeneity and delayed reproductive cell death [12, 13]. RIGI shows radiation dose and rate dependence [14] and can be detected following exposure to moderate doses of X-rays in multiple cell lines *in vitro* and in tissues of animals irradiated *in vivo* [10].

Genomic instability is present in the majority of cancers, driving tumor development and evolution. During tumor initiation, genomic instability has been proposed to accelerate the acquisition of mutations. There is evidence supporting the prevalence and role of genomic instability as a first step in the genesis of certain radiation-induced cancers *in vivo* [7, 15–18]. Thus, RIGI can be considered as a model to study inducible genomic instability and as a mechanism contributing to radiation-induced carcinogenesis [10].

Several factors have been shown to modulate RIGI. Oxidative stress associated with mitochondrial malfunction promotes a genomic instability state, as interference with reactive oxygen species generation or scavenging attenuates readouts [19]. Other factors that have been shown to influence RIGI are epigenetic changes and deficiencies in DNA repair [20–22]. However, no unifying molecular mechanism has been established for RIGI development yet.

In the current study we employ an immortalized, non-tumorigenic cell line of human bronchial epithelial cells HBEC3-KT, which have precursor properties as they can differentiate *in vitro* and can be progressed to further transformed states by oncogene expression or exposure to carcinogenic agents [23–25]. The lung is an organ remarkably susceptible to low doses of radiation [2, 26] and it is at high risk for carcinogenesis secondary to radiation therapy [27]. Irradiated HBEC3-KT reproduce several of the attributes and end points associated with RIGI. Our previous work showed that exposure to high and low LET radiation induced transient genomic instability peaking at day 7 and decreasing by days 14 and 21 post-irradiation [28, 29]. Phenotypes associated with genomic instability such as micronucleus formation and γH2AX and 53BP1 foci are cell autonomous at day 7. Micronucleus formation increases with dose, reaching saturation at 4Gy [30]. For the experiments in this work, two different cell lines, the bronchial epithelial cell line HBEC3-KT and the osteosarcoma cell line U2OS, were exposed to a 2Gy dose representing the average radiation dose per fraction received by patients during radiation therapy to identify cell type independent mechanisms. We leveraged the use of a panel of U2OS cell lines engineered to report the mechanism used to repair chromosomal breaks: homologous recombination (DRG), non-homologous end joining (EJ5) and alternative non-homologous end joining (EJ2) [31]. Employing protein arrays, we identify two potential mechanisms, replication stress and FOXM1, and evaluate their role in promoting two RIGI outcomes, micronucleus formation and homologous recombination.

Materials and methods

Cell lines, reagents and irradiations

The human bronchial epithelial cell line (HBEC3-KT) was a gift from Dr. Story (UT Southwestern), was authenticated by karyotyping and tested for mycoplasma at the moment of stock preparation. Cells were cultured in Keratinocyte serum free media (Invitrogen) supplemented with antibiotics, Epidermal growth Factor and Bovine Pituitary extract at 37˚C and 5%CO2. HBEC3-KT cells were transfected with Fugene HD or Lipofectamine 3000. FOXM1 and control aptamers were custom synthesized by Sigma with thio-modification, prepared and used at a 100nM concentration as described in [32]. U2OS were purchased from ATCC and grown in DMEM 7.5% FBS at 37˚C and 5% CO2. DRG, EJ5 and EJ2-U2OS cells were a gift from Dr. Jeremy Stark (Beckman Research Institute of the City of Hope) and were grown in DMEM 10% FBS at 37˚C and 5% CO2. At the moment of stock preparation, the cell lines were tested for mycoplasma and characterized by the SCE-1 transfection dependent increase in GFP positive cells and employing inhibitors or down regulating the expression of specific effectors in the DSB repair pathway [33]. The plasmid pCW57.1-FOXM1b was a gift from Adam Karpf (Addgene plasmid # 68811), pRRL sEF1a HA.NLS.Sce (opt).T2A.IFP was a gift from Andrew Scharenberg (Addgene plasmid # 31484).

Low-LET irradiation was carried out using an X-ray machine (X-RAD320, Precision X-Ray, N. Branford, CT, USA) at 320kV, 10mA. Irradiation was delivered at room temperature as a single dose of 320 kV X-rays (Precision X-Ray Inc., North Branford, CT, USA), at dose-rate approximately 2.3 Gy/min. For irradiations, 200 000 cells were plated in a T25 flask two days before irradiation in triplicates to ensure continuous proliferation before and after exposure. At day 4, each flask was subcultured at a1:3 ratio.

DNA repair reporter assay

At day 3 after irradiation, 500 000 cells of the reporter cell line were transfected with I-SceI IFP in triplicate. At day 6, all cells were incubated with 25μM biliverdin, and 18h later the cells were collected to measure expression of GFP and IFP (for transfection efficiency normalization) by flow cytometry in a FACS LSRII Instrument (BD Biosciences). The data collected was analyzed using FlowJo software as described [34]. Control and FOXM1 aptamer were transfected at 100nM at day 2 after irradiation.

Micronucleus assay

Cells were plated at a density of 20 000/well on glass coverslips and treated for 18h with 3 μg/ml Cytochalasin B in media to block cytokinesis before fixing with 4% PFA and staining with DAPI. Binucleated cells, which are the cells that underwent mitosis during the cytochalasin incubation period, were scored for the presence of micronuclei and/or nuclear blebs as previously described [28].

Reverse phase protein array

Cell lysates were prepared from three biological replicates in 50mM Hepes pH7.4, 1% Triton X-100, 150mM NaCl, 1.5mM MgCl$_2$, 1mM EGTA, 10% Glycerol containing anti proteases and anti phosphatases (Roche) and sent for analysis at the Reverse Phase Protein Array Core Facility at MD Anderson. Relative protein levels are obtained by interpolating several sample dilutions into a standard curve and then normalized for protein loading. The scatter plot was generated by graphing the difference between irradiated and non-irradiated averages of triplicate samples normalized and transformed to linear values. Included are only the proteins that

yielded a significant difference (paired t-test, $p<0.05$) in HBEC3-KT and/or U2OS cell lysates. Heat maps were generated with normalized log2 median centered data for each marker employing Morpheus software (Broad Institute).

DNA fiber assay

Cells were pulsed with 25μM IdU and then with 250μM CldU for 30 minutes each at 37˚C then released with trypsin and spotted on glass slides. DNA was spread following a 7min lysis with 0.5% SDS, 200 mM Tris-HCl pH 7.4, 50 mM EDTA. Dried slides were fixed with a (3:1) Methanol/Acetic acid mixture and denatured for 60min in 2.5 N HCl. Following 1h blocking in 15%FBS in PBS, the slides were incubated in primary antibodies for 2h 1:400 rat anti-bro-modeoxyuridine (ab6326 Abcam, AB_305426) and 1:50 mouse anti- bromodeoxyuridine (B44 BD, AB_2313824). After a stringency wash with 10 mM Tris–HCl pH 7.4, 400 mM NaCl, 0.2% Nonidet P40 (NP40), the slides were incubated with Alexafluor conjugated secondary antibodies: 488-conjugated chicken anti-rat, 488-conjugated goat anti-chicken, 594-conjugated rabbit anti-mouse and 594-conjugated goat anti-rabbit in 1:300 dilution. The slides were mounted in Fluoromount-G (Southern Biotech). Images of the fibers were acquired with a 63x oil immersion objective on a Zeiss Observer Z1 microscope equipped with Axiovision 4.8 software. 200 dual color labeled replication track length was measured employing Fiji Software and were converted to replication speed using a conversion factor of 2.59kb/μm [35, 36]. Statistical significance between groups was assessed using One Way ANOVA with a Bonferroni all pairs comparison post- test.

Real time quantitative PCR

Total RNA was isolated from Trizol solubilized cells and SuperScript III system (Invitrogen) was employed for cDNA synthesis. The relative standard curve method was employed following manufacturers protocol (QuantStudio 6, Applied Biosystems) to detect the expression of isoforms a, b and c and total FOXM1 employing previously published primers [37, 38] and irradiated HBEC3-KT samples to generate the standard curves. Non-irradiated samples were used as calibrators. For normalization we measured two housekeeping genes PCBP1 and RER1, which have been shown to have low variability in expression levels across a large number of samples [39].

Total FOXM1: 5'-acgtccccaagccaggctc-3' (forward), 5'-ctactgtagctcaggaataa-3' (reverse)
aFOXM1: 5'-tggggaacaggtggtgtttgg-3' (forward), 5'-gctagcagcactgataaacaaag-3' (reverse)
bFOXM1: 5'-ccaggtgtttaagcagcaga-3' (forward), 5'-tcctcagctagcagcaccttg-3' (reverse)
cFOXM1: 5'-caattgcccgagcacttggaatca-3' (forward), 5'-tcctcagctagcagcaccttg-3' (reverse)
PCBP1: 5'-tgatcatcgacaagctggag-3' (forward), 5'-tctttgatcttacacccgcc-3' (reverse)
RER1: 5'-cgtagcggagctgcgag-3' (forward), 5'-cgtgtagggtgtggacttgt-3' (reverse). FOXM1a amplification levels were too low to generate standard curves.

Immunofluorescence

RPA foci and anaphase bridges were detected in cells fixed with 4% paraformaldehyde and permeabilized with 0.2% TritonX-100. For RPA foci, cells were pre-extracted with 0.5% TritonX-100 before fixing. Antibodies used were RPA70 (NA13 Millipore Calbiochem AB_565121), 53BP1 (NB 100–304 Novus Biologicals AB_350221), Cyclin A (B-8 Santa Cruz AB_10709300). The slides were mounted in Fluoromount-G (Southern Biotech). Images were acquired with a 63x oil immersion objective on a Zeiss Observer Z1 microscope equipped with Axiovision 4.8 software. Images were processed using contrast/brightness enhancement only.

Foci were counted in at least 5 different fields totaling 50 or more cells in duplicate irradiations.

Western blot analysis

Cell lysates were preparing employing RIPA buffer (50mM Tris pH = 7.4, 150mM NaCl, 2mM EDTA, 0.5% NP40, 0.25% Sodium Deoxycholate) supplemented with Complete protease inhibitor and PHOSStop phosphatase inhibitor (Roche). Hundred micrograms of protein were separated in 10% SDS PAGE and transferred to a PVDF membrane. The membrane was probed with antibodies for FOXM1 (D12D5 AB_10692483), Cyclin B (D5C10 AB_2783553), CHK1 S345 (133D3 AB_331212) from CST, Rad51 (PC130 Calbiochem AB_2238184), Exo1 (ab95068 Abcam AB_10675762), RPA32 S4/S8 (A300-245A Bethyl AB_210547), GAPDH (GTX627408 GeneTex AB_11174761), tubulin (T6074 Sigma AB_477582). Bound antibodies were detected with infrared fluorescent secondary antibodies and imaged with a LI-COR Odyssey system. The numbers below the bands are fold of change over the non-treated condition calculated from the relative intensity of the bands quantified employing Image Studio Software.

Growth in soft agar

HBEC3-KT cells were irradiated in triplicate flasks and transfected at day 4 with the indicated DNA. At day 6, samples were collected to analyze for micronucleus formation. Cells were continuously passaged for 3 weeks. At week 4 media was changed to a 1:1 mixture of complete Keratinocyte Serum Free media and 10% FBS RPMI to accommodate potential metabolic changes and promote clone growth [40]. At the end of week 4, 50 000 cells per well were plated in 0.37% agar in triplicate wells over a 0.7% agar bottom layer. Colonies of a diameter larger than 10 cells were counted after 3 weeks.

Statistical analysis

The statistical test applied in each case is stated in the figure legend. Excel was used for two-tailed Student's t-test analysis assuming equal variance of the samples (type 2). Kaleidagraph (Synergy Software v 4.5) was used for One Way ANOVA employing a Bonferroni or Fisher's LSD post-hoc test as indicated in the figure legend. Statistical significance was defined at alpha level 0.05.

Results

We have previously shown that radiation induces transient genomic instability in HBEC3-KT cells expressed as increased micronuclei formation, residual 53BP1 and γH2AX foci, in the context of cellular oxidative stress [28]. To identify conserved mechanisms driving these phenotypes we leveraged RIGI development in two cell lines to exclude tissue specific mechanisms, we selected am immortalized nearly normal bronchial epithelial cell line HBEC3-KT and the osteosarcoma epithelial cell line U2OS, which has been widely used to study mechanism of DNA damage and repair because of DNA repair pathways and cell cycle regulation preservation [41, 42]. As shown in Fig 1A, following exposure to a 2Gy X-ray dose, a three-fold increase in micronucleus formation can be detected at day 7 in HBEC3-KT and at day 5 in U2OS, timing that corresponds to about 4 population doublings. The micronucleus assay detects fragments or whole chromosomes that can not engage with the mitotic spindle as a result of damage to chromosomes or the mitotic machinery (reviewed by M. Fenech [43]). Consistent with damaged DNA at the moment of mitosis, we measured four and two-fold
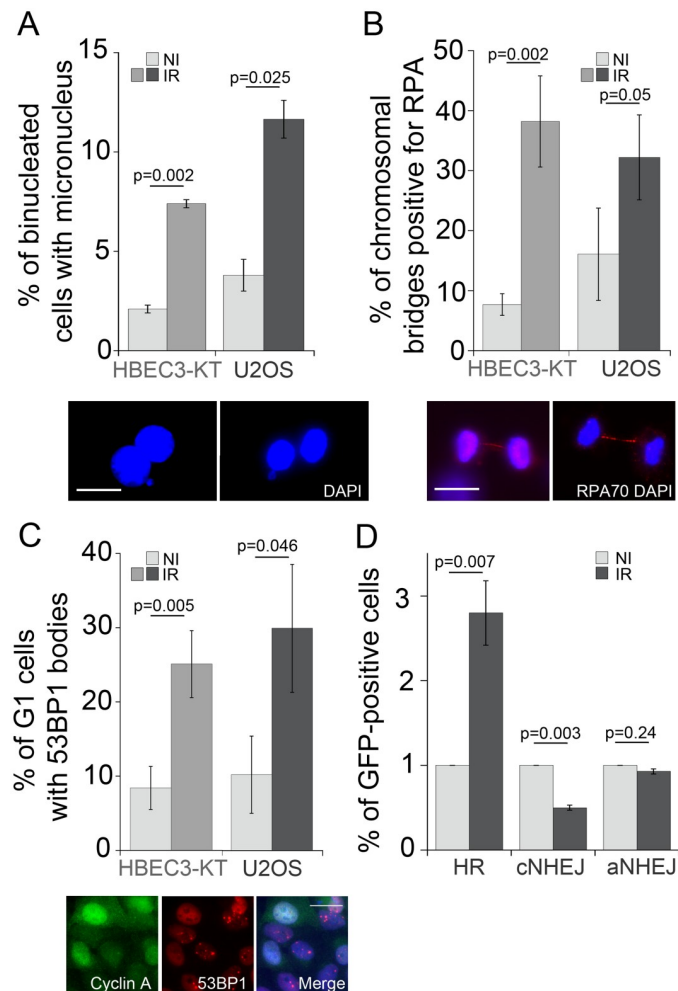
Fig 1. X-ray irradiated cells have damaged DNA at mitosis and increased usage of the HR pathway. A) Micronucleus formation rates at day 7 (HBEC3-KT) or day 5 (U2OS) following exposure to 2Gy X-ray. Average of 2 experiments, error bars represent SEM. Student's t-test. Inserts depict a representative image of binucleated HBEC3-KT cells with a micronucleus or a nuclear bud, respectively. Scale bar = 20μm. B) Increased frequency of RPA-positive chromosomal bridges in irradiated cells. Proliferating cultures of day 7 (HBEC3-KT) or day 5 (U2OS) following exposure to 2Gy X-ray were fixed and stained for RPA 70. An average of 90 mitosis per condition were scored for RPA positive bridges. Error bars represent standard deviation of triplicate samples. Student's t-test. Insert depicts a representative image of RPA-positive chromosomal bridge in U2OS (left panel) and HBEC3-KT (right panel) cells. Scale bar = 20μm. C) Frequency of nuclei with more than three 53BP1-positive foci per nuclei scored in an average of 100 Cyclin A negative nuclei per sample in HBEC3-KT at day 7 and in U2OS cells at day 5 following a 2Gy X-ray dose. Error bars represent standard deviation of triplicate samples. Student's t-test. Insert depicts HBEC3-KT cells with Cyclin A positive nuclei without 53BP1 bodies and Cyclin A negative nuclei with 53BP1 bodies. Scale bar = 20μm. D) Relative GFP induction levels in U2OS reporter cell lines for homologous recombination dependent repair (DRG), cNHEJ (EJ5) and aNHEJ (EJ2) at day 7 following exposure to a 2Gy X-ray dose. Average of 2 experiments, error bars represent SEM. Student's t-test.

increased frequency of Replication Protein A (RPA) positive chromosomal bridges in the irradiated cell populations for HBEC3-KT and U2OS respectively, an indication of single stranded DNA generation during genomic material segregation (Fig 1B). An additional reported consequence of DNA damage during mitosis is that 53BP1 bodies accumulate in the following G1 phase [44]. Both cell types showed roughly a three-fold increased accumulation of 53BP1 bodies in cells in G1 phase, identified by the absence of nuclear Cyclin A (Fig 1C). RPA positive

chromosomal bridges have been previously observed in cells that undergo mitosis in the presence of accumulated unresolved homologous recombination intermediaries [45, 46]. To test whether the homologous recombination repair pathway is used at a higher frequency in irradiated cells, we utilized a panel of genetically engineered U2OS cell lines with integrated GFP constructs to report the repair of a chromosomal DNA double strand break introduced by the endonuclease I-SceI by homologous recombination (HR), non-homologous end joining (c-NHEJ) and alternative non-homologous end joining (a-NHEJ) (Fig 1D and S1 Fig) [31]. Compared to non-irradiated cells, exposure to X-ray increased the number of GFP positive cells detected in the HR reporter line by 2.5 fold while the relative number of cells detected decreased in the c-NHEJ reporter line without affecting a-NHEJ dependent repair. Increased HR is a previously described RIGI outcome [47]. Altogether, these results suggest that several days following irradiation, replicating cells are undergoing mitosis with damaged DNA and relying more on the HR pathway to repair double strand breaks.

To gain further understanding of the mechanisms and scope of the alterations occurring in irradiated cells, we performed a functional proteomics analysis employing reverse phase protein arrays (RPPA) to assess the expression of 431 proteins including post-translational modifications relevant to cancer. Furthermore, this array is enriched in proteins involved in cell cycle regulation and HR. We analyzed the responses to a 2Gy dose X-ray at day 5 and 7 of HBEC3-KT cells and at day 5 for U2OS. Unsupervised hierarchical clustering of the results for HBEC3-KT show a clear segregation of the day 7 samples from the non irradiated and day 5 post-irradiation samples (S2 Fig), which is consistent with our previous findings that the phenotype at day 7 is a response that emerges overtime after exposure and not residual response to initial damage [29]. We reasoned that proteins and pathways that co-variate in both cell lines could be associated with common phenotypes induced by radiation exposure. A comparison between the proteins significantly differentially regulated in U2OS and HBEC3-KT (Fig 2A) reveals common up-regulation of phospho Aurora Kinase A and an increase in FOXM1 expression, a transcription factor that regulates the expression of multiple DNA repair proteins, increases HR dependent repair in the direct repeats conversion assay [48, 49] and cell cycle progression [50]. Analysis focused on proteins involved in cell cycle regulation and HR is shown in Fig 2B. The heat map exhibits an overall milder response for U2OS than HBEC3-KT cells, but both cell models display increased expression of markers related to end-resection (CtIP in U2OS and S4/S8 RPA phosphorylation in HBEC3-KT) in the context of small changes in levels and phosphorylation of proteins involved in checkpoint activation such as ATM, ATR, Chk1 and Chk2. The interrogation also reveals upregulation of proteins promoting M phase entry reflected by increases in CDK1 and Wee1 phosphorylation with increased PLK1 and Cdc25C, which are more prevalent in HBEC3-KT, but supported by a significant decrease in p21 expression in U2OS cells. In HBEC3-KT, RAD51 and Cyclin B, two targets for FOXM1 regulation, had increased expression at day 7. Collectively, these findings suggest the presence of a modest replication stress and checkpoint activation within the context of increased FOXM1 expression and activity.

To validate these findings, we measured DNA replication rate employing the DNA fiber assay. As shown in Fig 3A, replication speed was significantly slower (all doses vs. non irradiated p<0.0001, one way ANOVA) in cells that have been irradiated, reduced from 0.8 kb/min in non-irradiated cells to 0.61, 0.54 and 0.59 following doses of 2, 4 or 6 Gy. As the radiation dose increases, a larger fraction of the replication tracks become shorter, but the assay did not detect pausing or stalling as all tracks incorporated both labeled nucleotides and no significant track labeling asymmetry was detected (S3A Fig) [51]. As a reference, we measured a replication rate of 0.26 kb/min in cells treated with 25μM hydroxyurea for 24h. This low dose has been reported to cause replication stress by reducing the availability of nucleotides following
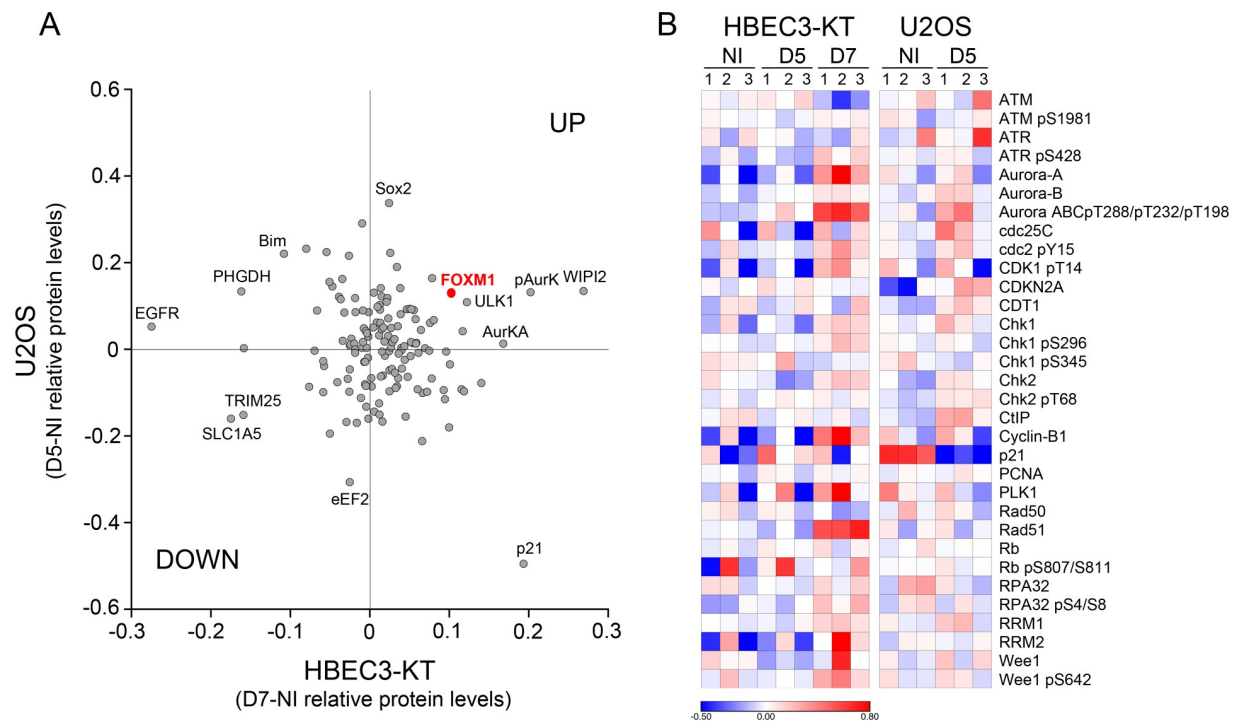
Fig 2. Reverse phase protein array analysis of proteins and post-translational modifications altered by exposure to X-ray. A) Scatterplot representing the relative protein level difference between irradiated and non-irradiated samples. Averages of triplicate samples normalized and transformed to linear values for each condition were subtracted. Each dot represents a protein that yielded a significant difference after irradiation (Student's t-test, $p < 0.05$) in cell lysates of HBEC3-KT at day 7 and/or U2OS at day 5. B) Heat map for proteins involved in cell cycle regulation and homologous recombination DNA repair pathway. The normalized log2 values for protein levels in each sample were median centered for each protein measured.

inhibition of ribonucleotide reductase [52]. Reduced replication speed leads to increased single stranded DNA accumulation, which binds RPA and commits damage repair by HR [53]. This prediction was examined by immunofluorescence to detect RPA associated with chromatin, which revealed that exposure to radiation increased by three-fold the percentage of cells with RPA foci in HBEC3-KT at day 7 and in U2OS at day 5 (Fig 3B). These results are consistent with increased RPA phosphorylation detected by RPPA (Fig 2B). Reduced availability of nucleotides is a mechanism leading to replication stress frequently found in cancer and can be reversed by nucleoside supplementation [54]. However, addition of nucleosides to the cultures in conditions that reduced micronucleus formation induced by HU was not effective in reducing radiation-induced effects (S3B Fig). We confirmed FOXM1 induction by western blot in lysates from both cell lines (Fig 3C). Interestingly, FOXM1 expression as well as RAD51 and EXO1, two genes that have been reported to be transcriptional targets for FOXM1 [55, 56] also increased in HBEC3-KT at day 7. U2OS cells have a higher basal FOXM1 expression, which was increased by radiation, but the up-regulation of the transcriptional targets measured was less robust than in HBEC3-KT cells. We sought next to identify the specific isoform induced by ionizing radiation by quantitative real time PCR employing specific primer pairs. In both cell lines, IR increased about two-fold total FOXM1 levels, mirroring the changes observed by western blot. Ionizing radiation increased the expression of isoform b in both cell types without affecting FOXM1c levels (Fig 3D).

Given the significant impact that FOXM1 expression has on the expression of DNA repair proteins and on carcinogenesis, we tested whether it is contributing to the genomic instability
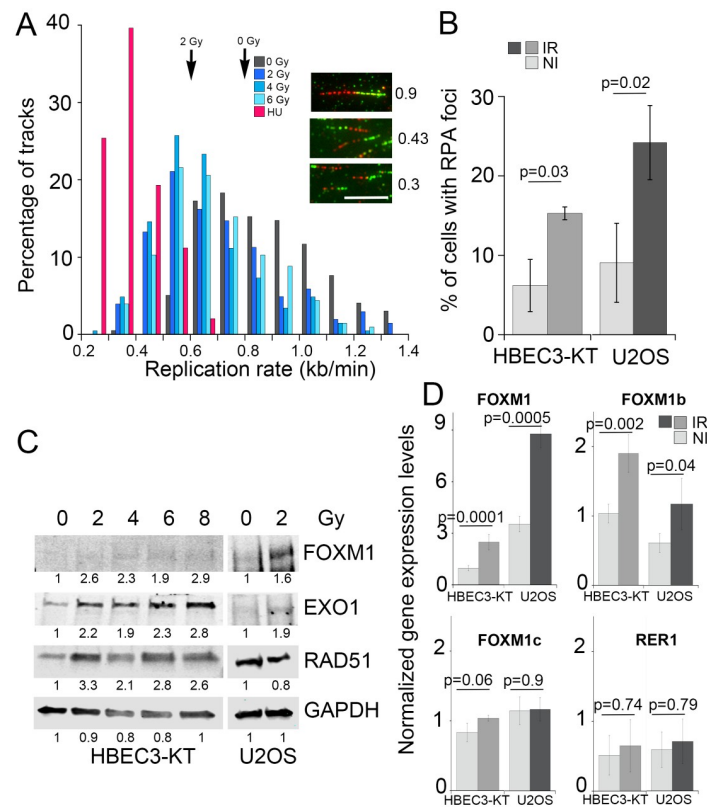
Fig 3. Irradiated cells have low levels of replication stress and induce FOXM1 expression. A) Frequency distribution plot of replication speed measured by the DNA fiber assay in HBEC3-KT cells at day 7 following exposure to the indicated X-ray doses. As a control, HBEC3-KT cells were treated for 48h with 25μM HU to reduce replication speed. Arrows indicate average speed. Inserts show examples of replication tracks of different length. Scale bar = 5μm. B) Quantification of the percentage of cells with RPA70 foci detected by immunofluorescence. Between 50 and 100 cells were scored in replicate samples of non-irradiated and day 7 irradiated HBEC3-KT cells or day 5 irradiated U2OS cells. Error bars represent standard deviation. Student's t-test. C) Western blot for FOXM1 expression and known transcriptional target proteins in HBEK3-KT at day 7 and in U2OS at day 5 post-exposure to the indicated X-ray dose. Numbers indicate ratio of signal of the lane over non-irradiated. D) Total FOXM1 and isoform b and c identification by Quantitative real time PCR analysis in HBEK3-KT at day 7 and in U2OS at day 5 post-exposure to 2 Gy X-ray dose. Gene expression levels of FOXM1 and a control gene (RER1) were normalized employing PCBP1 control gene. Error bars represent standard error of the mean of two experiments. Student's t-test.

https://doi.org/10.1371/journal.pone.0235998.g003

phenotypes in irradiated cells employing an aptamer oligonucleotide that was selected to interfere with transcriptional activity of FOXM1 (Aptamer) and compared to an oligomer of random sequence (Control) [32] instead of FOXM1 knockdown, because it has been shown that reduction in FOXM1 protein disrupts mitosis and causes DNA damage [57, 58]. The FOXM1-specific aptamer reduced the radiation-induced upregulation of EXO1, Cyclin B and RAD51 when delivered by transfection to HBEC3-KT cells (Fig 4A) without increasing micronucleus (Figs 4B and 6B) or HR (Fig 4C) in non-irradiated cells. The aptamer significantly reduced micronucleus formation rates in irradiated HBEC3-KT cells by 50% (Fig 4B), and reduced the number of GFP-positive cells resulting from homology-dependent repair in both irradiated and non-irradiated U2OS cells (Fig 4C). Taken together, these results suggest a role for FOXM1 in promoting RIGI in both cell types.

We tested next, whether FOXM1 overexpression is sufficient to induce some of the radiation-induced phenotypes. To increase FOXM1 expression levels we employed a cDNA construct regulated by Doxycycline (Fig 5A), which in U2OS cells increased the expression of
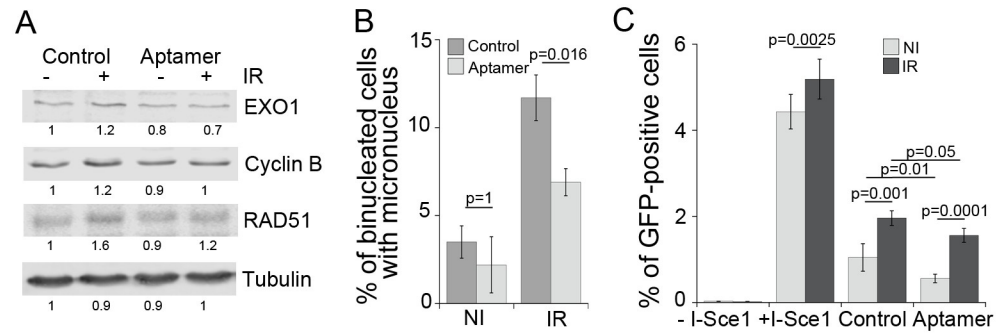
Fig 4. Interference with FOXM1 transcriptional activity reduces radiation induced phenotypes. A) Western blot analysis of known transcriptional target proteins for FOXM1 in HBEC3-KT at day 7 following exposure to 2Gy X-ray and transfection at day 3 with 100nM aptamer of random sequence (Control) or of a sequence interfering with FOXM1 transcriptional activity (Aptamer). B) Micronucleus assay in the same cells analyzed in A. Error bars represent standard deviation. 1 of 2 experiments shown. One Way ANOVA followed by Bonferroni post-test. C) Effect of aptamer transfection on the gene conversion assay to report homologous recombination dependent repair. Error bars represent SEM. Average of two experiments. One Way ANOVA followed by Bonferroni post-test.

EXO1 and RAD51 under our cell culture conditions even without Doxycycline addition. FOXM1b overexpression, but not empty vector, was sufficient to induce micronucleus formation in HBEC3-KT and U2OS (Fig 5B). FOXM1b overexpression, was sufficient to induce RPA phosphorylation in Serines 4 and 8, similar to the induction produced by a 48h treatment with 25μM HU or a 4h treatment with 3mM HU, conditions that induce mild and high replication stress, respectively (Fig 5C), consistent with previous reports [52]. FOXM1b overexpression also induced mild increases in CHK1phosphorylation, which is an indicator of checkpoint activation occurring as a response to disruptions in S phase. Collectively, these results indicate that FOXM1b expression alone induces replication stress as indicated by RPA and CHK1 phosphorylation and defects during mitosis measured by the micronucleus assay, reproducing some of the phenotypes induced by radiation.

The RPPA platform has been widely employed to analyze cell lines and tumor samples in the TCGA database and the results have been compiled in searchable databases [59, 60]. We asked next, how general is the correlation between FOXM1 expression and markers for replication stress (pS345 Chk1 and/or pS428 ATR) and FOXM1 transcriptional targets Cyclin B and RAD51 in cancer cell lines and tumor samples. A survey of the databases revealed that the cell lines derived from multiple cancer types show a significant (p<0.05) positive correlation of FOXM1 with Cyclin B and/or RAD51 expression suggesting FOXM1 activity, which did not necessarily correlate with average FOXM1 expression levels of each cancer type category (S4A and S4B Fig). The cell lines of 3 cancer types had a strong (R>0.66) and another 3 had a moderate (0.65>R>0.35) positive correlation between FOXM1 expression and a marker for replication stress. A significant positive correlation, although moderate (0.65>R>0.35) between FOXM1 and pS345 Chk1, is observed in tumor samples from liver, ovarian, cervical and testicular cancer (S5 Fig panel B). In tumor samples, liver, cervical and testicular tumors had higher levels of FOXM1 (S5 Fig panel A). These observations suggest that this is a mechanism highly represented in cancer lines and in a wide range of tumor types.

Given that our results show that radiation and FOXM1 induce replication stress, a known driver of cancer initiation and progression, we tested next whether exposure to radiation promotes cell transformation in HBEC3-KT and involves FOXM1 in this process. HBEC3-KT cells are immortalized but not transformed [23]. However, transformation and progression
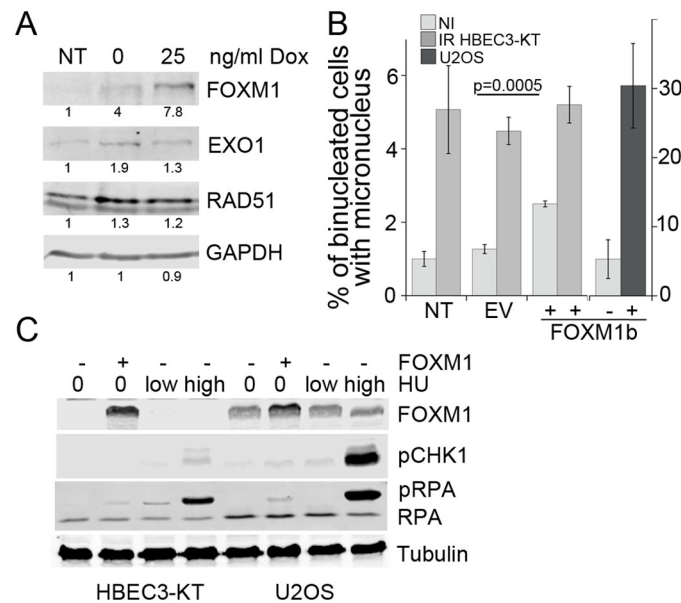
Fig 5. FOXM1b overexpression is sufficient to induce genomic instability. A) Western blot for Flag-tagged FOXM1 expression and transcriptional target proteins in stably expressing U2OS cells induced for 48h with the indicated Doxycycline concentration. B) Micronucleus formation in HBEC3-KT and U2OS transiently expressing FOXM1. Empty vector or FOXM1 were transfected 72h prior to the 18h incubation with cytochalasin. U2OS cells were treated with 1µg/ml Dox. Error bars represent SEM. Student's t-test. C) Western blot analysis for RPA2 and Chk1 phosphorylation in HBEC3-KT and U2OS cells overexpressing FOXM1 or treated with HU 25µM for 48h or 3mM for 4h.

towards malignancy can be induced by exposure to carcinogens such as radiation, and cigarette smoke condensate [61, 62] and by expression of several oncogenes [63]. As an intermediate step in transformation and progression, HBEC3-KT cells acquire the capability to form colonies in soft agar, which measures anchorage independent growth. Cell cultures were irradiated in triplicate with a 4 Gy dose to increase the sensitivity of the assay by inducing a greater response measured by reduced DNA replication (Fig 3A) and higher levels of micronuclei formation (Fig 6A) [30]. At day 7, the effects of the different treatments were evaluated by micronucleus formation shown in Fig 6A. At 4 weeks of continuous growth, the cells were evaluated for the capability to grow in soft agar. Exposure to radiation significantly increased the number of colonies in mock and in control aptamer transfected cells. Transient interference with FOXM1 activity at the time of genomic instability by the aptamer, reduced the radiation response, demonstrating a role for both, RIGI and FOXM1 activity on cell transformation events. All together these results suggest that low levels of FOXM1 activity, such as the ones induced by radiation exposure, are sufficient to promote cell transformation.

Discussion

In this work we have uncovered two mechanisms, replication stress and FOXM1 expression, driving RIGI following exposure to X-rays. We employed functional proteomics to evaluate the expression of a selected number of proteins in two cell lines, HBEC3-KT and U2OS, exhibiting RIGI at days 7 and 5 post-irradiation respectively. The signature of changes detected indicated the presence of replication stress and implicated FOXM1 as a candidate molecule to promote RIGI. These predictions were confirmed by measuring slower DNA replication rates with the DNA fiber assay and accumulation of ssDNA in irradiated cells as well as by
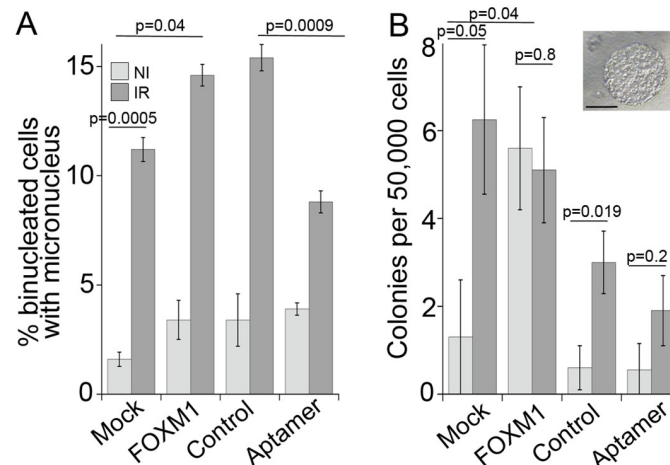
Fig 6. FOXM1 expression promotes cell transformation. Triplicate flasks of HBEC3-KT cells were exposed to 4Gy X-ray and transfected at day 4 with the indicated construct. At day 6 post-irradiation, the cells were passaged and samples were collected for micronucleus assay shown in (A). After a month of continuous growth, the cells were tested for growth in soft agar shown in (B). Error bars represent SEM. Student's t-test and One Way ANOVA with Fisher's LSD post-test for aptamer and radiation samples. Scale bar = 200 μm.

modifying RIGI outcomes by altering FOXM1 activity. Furthermore, employing these tools to interfere with delayed genomic instability, we demonstrate a contribution of RIGI to radiation-induced cell transformation of HBRC3-KT cells *in vitro*.

One of our most significant finding is replication stress in cells undergoing RIGI, which mechanistically may explain several of the outcomes associated with RIGI measured in previous studies and add novel outcomes to further describe this non-targeted effect. Employing the DNA fiber assay, we detected lower replication elongation rates in irradiated cells, slowing down as the dose of the initial exposure increases (Fig 3A). Reduced processivity of the replication machinery is known to be sufficient to cause uncoupling with replicative helicases, exposing RPA-binding ssDNA [64], which we detected as increased RPA-positive foci (Fig 3B). HR (Fig 1D) is activated as a tolerance mechanism to repair DNA DSBs that are more prone to occur and to stabilize and repair replication forks [65] and is a RIGI outcome following low and high LET radiation exposures [47]. An additional consequence of reduced replication speed is the incomplete replication of the genome, particularly in late replicating regions rich in chromosomal fragile sites or of low density in replication origins [66]. Non-replicated regions result in nondisjunction of sister chromatids during mitosis, which leads to the formation of anaphase bridges [67], often exposing ssDNA, which we detected as RPA-positive bridges (Fig 1B). RPA positive chromosomal bridges, associated with chromosomal aberrations, are observed when replication stress is induced in cancer cells [54]. DNA damaged during mitosis is protected by 53BP1 binding until repair during the following phase of the cell cycle [44], which we measured in irradiated cultures as an increased frequency of 53BP1 bodies in Cyclin A-negative cells (Fig 1C). A screen to identify factors contributing to the formation of 53BP1 bodies found that the most effective condition was a low aphidicolin dose, sufficient to impair replication fork progression through physiological barriers [68], supporting the notion that a reduction in replication elongation rate such as the observed in our work, would be sufficient to induce all these RIGI phenotypes [44]. Replication stress could also explain additional RIGI outcomes previously described in the literature but not investigated in this work: Slow or arrested replication forks stimulate the use of potentially mutagenic DNA repair

pathways that can lead to the accumulation of mutations and to chromosomal rearrangements (reviewed by Gaillard et. al [64]). Replication stress induces DSB formation and ssDNA gaps which lead to chromosomal fragility and gap formation at metaphase [54]. Increased HR activity is associated with increased sister-chromatid exchanges and recombination events (reviewed in [69]).

The main causes for replication stress have been attributed to the reduced availability of resources required for replication, including nucleotides or histones as well as structural impediments in the DNA, such as damage, bound proteins or DNA secondary structures [70]. We examined whether a deficiency in the nucleotide pool was a factor, which is a common mechanism leading to replication stress in oncogene-driven cancer [54], however increasing the availability of nucleotides had no effect (S3B Fig). Another factor affecting replication rate could be chronic oxidative stress, which we have previously shown to be present in HBEC3-KT at day 7-post irradiation [28]. Chronic oxidative stress has been shown to slow replication in HR defective cells, however this deficiency can be suppressed by supplying nucleotide precursors [71]. Low levels of ROS have been shown to induce the dissociation of the component of the replication protection complex Timeless, from the replisome causing fork slowdown [72] and the modification of several other factors involved in replication [70]. However, our previous characterization of the oxidative stress response in these cells indicates that oxidative stress is a permissive factor for genomic instability engaged at low dose, while many of the genomic instability readouts show dose dependency pointing to an additional determinant factor [28, 30].

We identified FOXM1 as a second factor modulating RIGI outcomes. FOXM1 is a transcription factor widely expressed in pre-malignant lesions and cancer, and is included in a chromosomal instability signature correlating with functional aneuploidy and highly predictive for clinical outcomes [73, 74]. Our findings are consistent with FOXM1 activity promoting genomic instability. We show that radiation increased FOXM1b expression with dose at day 7 post-exposure (Fig 3C and 3D) and that FOXM1b overexpression is sufficient to induce RPA and Chk1 phosphorylation (Fig 5C), considered as the most specific indicators for replication stress [75, 76]. While the induced phosphorylation levels were small, they were comparable to low doses of HU, which we show reduced replication rate and increased micronucleus formation (S3 Fig). Low doses of aphidicolin or HU are sufficient to reduce replication speed without significant ATR and Chk1 activation [52, 77] have been also shown to induce 53BP1bodies optimally [44] and expression of CFS [68]. Replication stress would offer a mechanism to explain reported FOXM1 dependent increases in LOH, and CNV [78, 79], which have been also identified as RIGI outcomes. Interference with FOXM1 transcriptional activity reduced radiation-induced micronucleus formation and increased HR dependent repair, while overexpression was sufficient to induce micronuclei formation (Figs 4 and 5).

FOXM1 controls the expression of multiple genes involved in DNA homeostasis including NBS, BRIP1, XRCC1, BRCA2, EXO1, RAD51 and RRM2 as well as cell cycle regulation, Cyclin B and PLK1 [48, 49, 55, 56, 58, 80, 81] and reviewed in [50]. Several of these targets could mediate FOXM1 role during RIGI. Overexpression of RAD51 increases HR activity and chromosomal instability [82], and overexpressed EXO1 promotes end resection [83]. An alternative mechanism could be by promotion of premature entry into mitosis by inducing the expression of Cyclin B and PLK1 [57]. Given these pleiotropic effects, further experiments beyond the scope of this work, are needed to identify the transcriptional target of FOXM1 promoting RIGI.

We show evidence supporting a role for FOXM1 in radiation-induced cell transformation as transient interference with FOXM1 transcriptional activity was sufficient to dampen cell growth in soft agar induced by IR (Fig 6B). This activity is consistent with transgenic mice

models showing that FOXM1 expression promotes early steps in tumorigenesis, promoting Clara cell and hepatocyte hyperplasia for example [84, 85] and acting in conjunction with many other carcinogens [86] as well as cancer cell lines [87, 88]. Replication stress has been shown to be a source for genomic instability in pre-neoplasic lesions, while in normal cells replication stress leads to cell death or senescence through activation of DDR [89–91]. FOXM1 expression could be a tolerance mechanism to evade anti-proliferative signals, such as oncogene-induced differentiation [92], DNA damage-induced senescence [49] and aging [93], and allow the proliferation of genomically unstable cells. Thus, we propose that FOXM1 expression is enabling radiation induced cell transformation.

In summary, we show that HBEC3-KT is a model system to elucidate mechanisms driving RIGI, as it reproduces many of the outcomes for RIGI reported in other model systems. Moreover, by transient interference with FOXM1 activity, we demonstrate that the observed transient increase in genomic instability contributes to radiation-induced cell transformation and is thus a potential target of intervention to mitigate late emerging deleterious effects of radiation exposure.

Supporting information

S1 Fig. Detail of the constructs engineered in U2OS cells to report the repair of a double strand break introduced by cleavage with the endonuclease I-SceI. GFP expression is gained when repair occurs by the specific mechanism.
(TIF)

S2 Fig. Heat Map of the relative expression of all the antigens profiled by the reverse phase protein array after hierarchical clustering. Triplicate samples of non-irradiated (NI) or 2Gy irradiated HBEC3-KT cell lysates collected at day 5 or day 7. Heat map represents "rank-ordered" changes induced by each treatment, calculated by summing median-centered normalized protein amount.
(TIF)

S3 Fig. Characterization of radiation induced replication stress. A) Asymmetry of replication track: the graph depicts the ratio of CldU/IdU track length for each dose. No statistical divergence following One Way ANOVA analysis. B) Micronucleus formation rates in HBEC3-KT or U2OS cells were irradiated or treated for 48h with 25μM HU with or without 30μM nucleosides. Error bars are SEM. Student' t-test.
(TIF)

S4 Fig. Correlation of FOXM1 expression with transcriptional targets and replication stress marker levels in cancer cell lines samples analyzed with the RPPA platform. A) Relative FOXM1 expression across datasets of cell lines grouped by cancer type extracted from the MD Anderson Cell Lines Project Portal. https://tcpaportal.org/mclp/#/ B) Table listing the correlation factor and significance of paired comparison of the indicated protein with FOXM1 expression in each dataset of cell lines grouped by cancer types. Included are the comparisons that were significant (p≤ 0.05).
(TIF)

S5 Fig. Correlation of FOXM1 expression with transcriptional targets and replication stress marker levels in tumor samples analyzed with the RPPA platform. A) Relative FOXM1 expression across datasets of tumor samples grouped by cancer type extracted from the The Cancer Proteome Atlas. https://tcpaportal.org/tcpa/. B) Table listing the correlation factor and significance of paired comparison of the indicated protein with FOXM1 expression

in each dataset of tumor samples grouped by cancer types. Included are the comparisons that were significant (p≤ 0.05).
(TIF)

S1 Raw images. Uncropped gel images.
(TIF)

Acknowledgments

Author Contributions

Conceptualization: Erica Werner.

Funding acquisition: Paul W. Doetsch, Erica Werner.

Investigation: Zhentian Li, Erica Werner.

Resources: David S. Yu.

Writing – original draft: Zhentian Li, Erica Werner.

Writing – review & editing: Zhentian Li, David S. Yu, Paul W. Doetsch, Erica Werner.

References

1. Delaney GP, Barton MB. Evidence-based estimates of the demand for radiotherapy. Clin Oncol (R Coll Radiol). 2015; 27(2):70–76.

2. Suit H, Goldberg S, Niemierko A, Ancukiewicz M, Hall E, Goitein M, et al. Secondary carcinogenesis in patients treated with radiation: a review of data on radiation-induced cancers in human, non-human primate, canine and rodent subjects. Radiat Res. 2007; 167(1):12–42. https://doi.org/10.1667/RR0527.1 PMID: 17214511

3. Berrington de Gonzalez A, Curtis RE, Kry SF, Gilbert E, Lamart S, Berg CD, et al. Proportion of second cancers attributable to radiotherapy treatment in adults: a cohort study in the US SEER cancer registries. Lancet Oncol. 2011; 12(4):353–360. https://doi.org/10.1016/S1470-2045(11)70061-4 PMID: 21454129

4. Braunstein S, Nakamura JL. Radiotherapy-induced malignancies: review of clinical features, pathobiology, and evolving approaches for mitigating risk. Frontiers in oncology. 2013; 3:73. https://doi.org/10.3389/fonc.2013.00073 PMID: 23565507

5. Sherborne AL, Davidson PR, Yu K, Nakamura AO, Rashid M, Nakamura JL. Mutational Analysis of Ionizing Radiation Induced Neoplasms. Cell Rep. 2015; 12(11):1915–1926. https://doi.org/10.1016/j.celrep.2015.08.015 PMID: 26344771

6. Lee CL, Mowery YM, Daniel AR, Zhang D, Sibley AB, Delaney JR, et al. Mutational landscape in genetically engineered, carcinogen-induced, and radiation-induced mouse sarcoma. JCI Insight. 2019; 4(13).

7. Little JB. Radiation carcinogenesis. Carcinogenesis. 2000; 21(3):397–404. https://doi.org/10.1093/carcin/21.3.397 PMID: 10688860

8. Shibata AA-O, Jeggo PA-O. A historical reflection on our understanding of radiation-induced DNA double strand break repair in somatic mammalian cells; interfacing the past with the present. International Journal of Radiation Biology. 2019; 95(5):945–956. https://doi.org/10.1080/09553002.2018.1564083 PMID: 30608893

9. Jackson SP, Bartek J. The DNA-damage response in human biology and disease. Nature. 2009; 461 (7267):1071–1078. https://doi.org/10.1038/nature08467 PMID: 19847258

10. Morgan WF. Non-targeted and delayed effects of exposure to ionizing radiation: II. Radiation-induced genomic instability and bystander effects in vivo, clastogenic factors and transgenerational effects. Radiat Res. 2003; 159(5):581–596. https://doi.org/10.1667/0033-7587(2003)159[0581:nadeoe]2.0.co;2 PMID: 12710869

11. Kadhim M, Salomaa S, Wright E, Hildebrandt G, Belyakov OV, Prise KM, et al. Non-targeted effects of ionising radiation–implications for low dose risk. Mutat Res. 2013; 752(2):84–98. https://doi.org/10.1016/j.mrrev.2012.12.001 PMID: 23262375

12. Morgan WF, Day JP, Kaplan MI, McGhee EM, Limoli CL. Genomic instability induced by ionizing radiation. Radiat Res. 1996; 146(3):247–258. PMID: 8752302

13. Flunkert J, Maierhofer A, Dittrich M, Müller T, Horvath S, Nanda I, et al. Genetic and epigenetic changes in clonal descendants of irradiated human fibroblasts. Experimental cell research. 2018; 370(2):322–332. https://doi.org/10.1016/j.yexcr.2018.06.034 PMID: 29964050

14. Elbakrawy EM, Hill MA, Kadhim MA. Radiation-induced Chromosome Instability: The Role of Dose and Dose Rate. Genome integrity. 2019; 10:3. https://doi.org/10.4103/genint.genint_5_19 PMID: 31897286

15. Ullrich RL, Ponnaiya B. Radiation-induced instability and its relation to radiation carcinogenesis. Int J Radiat Biol. 1998; 74(6):747–754. https://doi.org/10.1080/095530098141023 PMID: 9881720

16. Yahyapour R, Salajegheh A, Safari A, Amini P, Rezaeyan A, Amraee A, et al. Radiation-induced Non-targeted Effect and Carcinogenesis; Implications in Clinical Radiotherapy. Journal of Biomedical Physics and Engineering. 2018; 8(4):435–446. PMID: 30568933

17. Biermann J, Langen B, Nemes S, Holmberg E, Parris TZ, Werner Rönnerman E, et al. Radiation-induced genomic instability in breast carcinomas of the Swedish hemangioma cohort. Genes, chromosomes & cancer. 2019; 58(9):627–635. https://doi.org/10.1002/gcc.22757 PMID: 30938900

18. Oikawa M, Yoshiura K, Kondo H, Miura S, Nagayasu T, Nakashima M. Significance of genomic instability in breast cancer in atomic bomb survivors: analysis of microarray-comparative genomic hybridization. Radiation oncology (London, England). 2011; 6:168. https://doi.org/10.1186/1748-717X-6-168 PMID: 22152285

19. Kim GJ, Chandrasekaran K, Morgan WF. Mitochondrial dysfunction, persistently elevated levels of reactive oxygen species and radiation-induced genomic instability: a review. Mutagenesis. 2006; 21 (6):361–367. https://doi.org/10.1093/mutage/gel048 PMID: 17065161

20. Baulch JE, Aypar U, Waters KM, Yang AJ, Morgan WF. Genetic and epigenetic changes in chromosomally stable and unstable progeny of irradiated cells. PLoS One. 2014; 9(9):e107722. https://doi.org/10.1371/journal.pone.0107722 PMID: 25251398

21. Yu Y, Okayasu R, Weil MM, Silver A, McCarthy M, Zabriskie R, et al. Elevated breast cancer risk in irradiated BALB/c mice associates with unique functional polymorphism of the Prkdc (DNA-dependent protein kinase catalytic subunit) gene. Cancer Res. 2001; 61(5):1820–1824. PMID: 11280730

22. Baulch JE. Radiation-induced genomic instability, epigenetic mechanisms and the mitochondria: a dysfunctional ménage a trois? Int J Radiat Biol. 2019; 95(4):516–525. https://doi.org/10.1080/09553002.2018.1549757 PMID: 30451575

23. Ramirez RD, Sheridan S, Girard L, Sato M, Kim Y, Pollack J, et al. Immortalization of human bronchial epithelial cells in the absence of viral oncoproteins. Cancer Res. 2004; 64(24):9027–9034. https://doi.org/10.1158/0008-5472.CAN-04-3703 PMID: 15604268

24. Delgado O, Kaisani AA, Spinola M, Xie XJ, Batten KG, Minna JD, et al. Multipotent capacity of immortalized human bronchial epithelial cells. PLoS One. 2011; 6(7):e22023. https://doi.org/10.1371/journal.pone.0022023 PMID: 21760947

25. Sato M, Larsen JE, Lee W, Sun H, Shames DS, Dalvi MP, et al. Human lung epithelial cells progressed to malignancy through specific oncogenic manipulations. Mol Cancer Res. 2013; 11(6):638–650. https://doi.org/10.1158/1541-7786.MCR-12-0634-T PMID: 23449933

26. Ron E. Cancer risks from medical radiation. Health Phys. 2003; 85(1):47–59. https://doi.org/10.1097/00004032-200307000-00011 PMID: 12852471

27. Kumar S. Second malignant neoplasms following radiotherapy. Int J Environ Res Public Health. 2012; 9 (12):4744–4759. https://doi.org/10.3390/ijerph9124744 PMID: 23249860

28. Werner E, Wang H, Doetsch PW. Opposite roles for p38MAPK-driven responses and reactive oxygen species in the persistence and resolution of radiation-induced genomic instability. PLoS One. 2014; 9 (10):e108234. https://doi.org/10.1371/journal.pone.0108234 PMID: 25271419

29. Werner E, Wang Y, Doetsch PW. A Single Exposure to Low- or High-LET Radiation Induces Persistent Genomic Damage in Mouse Epithelial Cells In Vitro and in Lung Tissue. Radiat Res. 2017; 188(4):373–380. https://doi.org/10.1667/RR14685.1 PMID: 28753066

30. Werner E, Wang H, Doetsch PW. Role of Pro-inflammatory Cytokines in Radiation-Induced Genomic Instability in Human Bronchial Epithelial Cells. Radiat Res. 2015; 184(6):621–629. https://doi.org/10.1667/RR14045.1 PMID: 26579942

31. Bennardo N, Cheng A, Huang N, Stark JM. Alternative-NHEJ is a mechanistically distinct pathway of mammalian chromosome break repair. PLoS Genet. 2008; 4(6):e1000110. https://doi.org/10.1371/journal.pgen.1000110 PMID: 18584027

32. Xiang Q, Tan G, Jiang X, Wu K, Tan W, Tan Y. Suppression of FOXM1 Transcriptional Activities via a Single-Stranded DNA Aptamer Generated by SELEX. Sci Rep. 2017; 7:45377. https://doi.org/10.1038/srep45377 PMID: 28358012

33. Daly M.B.; Minten E.V.; Whelan D.R.; Schlafstein A.J.; Zhang H.; Amand R.; et al. SAMHD1 Promotes DNA End Resection to facilitate DNA Repair by Homologous Recombination. Cell Reports. 2017; 20 (8):1921–1935. https://doi.org/10.1016/j.celrep.2017.08.008 PMID: 28834754

34. Li Z, Hudson FZ, Wang H, Wang Y, Bian Z, Murnane JP, et al. Increased mutagenic joining of enzymatically-induced DNA double-strand breaks in high-charge and energy particle irradiated human cells. Radiat Res. 2013; 180(1):17–24. https://doi.org/10.1667/RR3332.1 PMID: 23692479

35. Jackson DA, Pombo A. Replicon clusters are stable units of chromosome structure: evidence that nuclear organization contributes to the efficient activation and propagation of S phase in human cells. J Cell Biol. 1998; 140(6):1285–1295. https://doi.org/10.1083/jcb.140.6.1285 PMID: 9508763

36. Daigaku Y, Davies AA, Ulrich HD. Ubiquitin-dependent DNA damage bypass is separable from genome replication. Nature. 2010; 465(7300):951–955. https://doi.org/10.1038/nature09097 PMID: 20453836

37. Kong X, Li L, Li Z, Le X, Huang C, Jia Z, et al. Dysregulated expression of FOXM1 isoforms drives progression of pancreatic cancer. Cancer Res. 2013; 73(13):3987–3996. https://doi.org/10.1158/0008-5472.CAN-12-3859 PMID: 23598278

38. Barger CJ, Zhang W, Hillman J, Stablewski AB, Higgins MJ, Vanderhyden BC, et al. Genetic determinants of FOXM1 overexpression in epithelial ovarian cancer and functional contribution to cell cycle progression. Oncotarget. 2015; 6(29):27613–27627. https://doi.org/10.18632/oncotarget.4546 PMID: 26243836

39. Jo J, Choi S, Oh J, Lee SG, Choi SY, Kim KK, et al. Conventionally used reference genes are not outstanding for normalization of gene expression in human cancer research. BMC Bioinformatics. 2019; 20 (Suppl 10):245. https://doi.org/10.1186/s12859-019-2809-2 PMID: 31138119

40. Hamburger AW, White CP, Dunn FE, Citron ML, Hummel S. Modulation of human tumor colony growth in soft agar by serum. Int J Cell Cloning. 1983; 1(4):216–229. https://doi.org/10.1002/stem.5530010403 PMID: 6366083

41. Lukas C, Falck J, Bartkova J, Bartek J, Lukas J. Distinct spatiotemporal dynamics of mammalian checkpoint regulators induced by DNA damage. Nat Cell Biol. 2003; 5(3):255–260. https://doi.org/10.1038/ncb945 PMID: 12598907

42. Adamson B, Smogorzewska A, Sigoillot FD, King RW, Elledge SJ. A genome-wide homologous recombination screen identifies the RNA-binding protein RBMX as a component of the DNA-damage response. Nat Cell Biol. 2012; 14(3):318–328. https://doi.org/10.1038/ncb2426 PMID: 22344029

43. Fenech M. Cytokinesis-block micronucleus cytome assay. Nat Protoc. 2007; 2(5):1084–1104. https://doi.org/10.1038/nprot.2007.77 PMID: 17546000

44. Lukas C, Savic V, Bekker-Jensen S, Doil C, Neumann B, Pedersen RS, et al. 53BP1 nuclear bodies form around DNA lesions generated by mitotic transmission of chromosomes under replication stress. Nat Cell Biol. 2011; 13(3):243–253. https://doi.org/10.1038/ncb2201 PMID: 21317883

45. Fernandez-Casanas M, Chan KL. The Unresolved Problem of DNA Bridging. Genes (Basel). 2018; 9 (12). https://doi.org/10.3390/genes9120623 PMID: 30545131

46. Chan YW, Fugger K, West SC. Unresolved recombination intermediates lead to ultra-fine anaphase bridges, chromosome breaks and aberrations. Nat Cell Biol. 2018; 20(1):92–103. https://doi.org/10.1038/s41556-017-0011-1 PMID: 29255170

47. Allen CP, Hirakawa H, Nakajima NI, Moore S, Nie J, Sharma N, et al. Low- and High-LET Ionizing Radiation Induces Delayed Homologous Recombination that Persists for Two Weeks before Resolving. Radiat Res. 2017; 188(1):82–93. https://doi.org/10.1667/RR14748.1 PMID: 28535128

48. Monteiro LJ, Khongkow P, Kongsema M, Morris JR, Man C, Weekes D, et al. The Forkhead Box M1 protein regulates BRIP1 expression and DNA damage repair in epirubicin treatment. Oncogene. 2013; 32(39):4634–4645. https://doi.org/10.1038/onc.2012.491 PMID: 23108394

49. Khongkow P, Karunarathna U, Khongkow M, Gong C, Gomes AR, Yague E, et al. FOXM1 targets NBS1 to regulate DNA damage-induced senescence and epirubicin resistance. Oncogene. 2014; 33 (32):4144–4155. https://doi.org/10.1038/onc.2013.457 PMID: 24141789

50. Nestal de Moraes G, Bella L, Zona S, Burton MJ, Lam EW. Insights into a Critical Role of the FOXO3a-FOXM1 Axis in DNA Damage Response and Genotoxic Drug Resistance. Curr Drug Targets. 2016; 17 (2):164–177. https://doi.org/10.2174/1389450115666141122211549 PMID: 25418858

51. Techer H, Koundrioukoff S, Azar D, Wilhelm T, Carignon S, Brison O, et al. Replication dynamics: biases and robustness of DNA fiber analysis. J Mol Biol. 2013; 425(23):4845–4855. https://doi.org/10.1016/j.jmb.2013.03.040 PMID: 23557832

52. Koundrioukoff S, Carignon S, Techer H, Letessier A, Brison O, Debatisse M. Stepwise activation of the ATR signaling pathway upon increasing replication stress impacts fragile site integrity. PLoS Genet. 2013; 9(7):e1003643. https://doi.org/10.1371/journal.pgen.1003643 PMID: 23874235

53. Ceccaldi R, Rondinelli B, D'Andrea AD. Repair Pathway Choices and Consequences at the Double-Strand Break. Trends in Cell Biology. 2016; 26(1):52–64. https://doi.org/10.1016/j.tcb.2015.07.009 PMID: 26437586

54. Burrell RA, McClelland SE, Endesfelder D, Groth P, Weller MC, Shaikh N, et al. Replication stress links structural and numerical cancer chromosomal instability. Nature. 2013; 494(7438):492–496. https://doi.org/10.1038/nature11935 PMID: 23446422

55. Zhang N, Wu X, Yang L, Xiao F, Zhang H, Zhou A, et al. FoxM1 inhibition sensitizes resistant glioblastoma cells to temozolomide by downregulating the expression of DNA-repair gene Rad51. Clin Cancer Res. 2012; 18(21):5961–5971. https://doi.org/10.1158/1078-0432.CCR-12-0039 PMID: 22977194

56. Zhou J, Wang Y, Wang Y, Yin X, He Y, Chen L, et al. FOXM1 modulates cisplatin sensitivity by regulating EXO1 in ovarian cancer. PLoS One. 2014; 9(5):e96989. https://doi.org/10.1371/journal.pone.0096989 PMID: 24824601

57. Laoukili J, Kooistra MR, Bras A, Kauw J, Kerkhoven RM, Morrison A, et al. FoxM1 is required for execution of the mitotic programme and chromosome stability. Nat Cell Biol. 2005; 7(2):126–136. https://doi.org/10.1038/ncb1217 PMID: 15654331

58. Tan Y, Raychaudhuri P, Costa RH. Chk2 mediates stabilization of the FoxM1 transcription factor to stimulate expression of DNA repair genes. Mol Cell Biol. 2007; 27(3):1007–1016. https://doi.org/10.1128/MCB.01068-06 PMID: 17101782

59. Li J, Lu Y, Akbani R, Ju Z, Roebuck PL, Liu W, et al. TCPA: a resource for cancer functional proteomics data. Nat Methods. 2013; 10(11):1046–1047. https://doi.org/10.1038/nmeth.2650 PMID: 24037243

60. Li J, Zhao W, Akbani R, Liu W, Ju Z, Ling S, et al. Characterization of Human Cancer Cell Lines by Reverse-phase Protein Arrays. Cancer Cell. 2017; 31(2):225–239. https://doi.org/10.1016/j.ccell.2017.01.005 PMID: 28196595

61. Ding LH, Park S, Xie Y, Girard L, Minna JD, Story MD. Elucidation of changes in molecular signalling leading to increased cellular transformation in oncogenically progressed human bronchial epithelial cells exposed to radiations of increasing LET. Mutagenesis. 2015; 30(5):685–694. https://doi.org/10.1093/mutage/gev028 PMID: 26001755

62. Vaz M, Hwang SY, Kagiampakis I, Phallen J, Patil A, O'Hagan HM, et al. Chronic Cigarette Smoke-Induced Epigenomic Changes Precede Sensitization of Bronchial Epithelial Cells to Single-Step Transformation by KRAS Mutations. Cancer Cell. 2017; 32(3):360–376 e366. https://doi.org/10.1016/j.ccell.2017.08.006 PMID: 28898697

63. Sato M, Vaughan MB, Girard L, Peyton M, Lee W, Shames DS, et al. Multiple oncogenic changes (K-RAS(V12), p53 knockdown, mutant EGFRs, p16 bypass, telomerase) are not sufficient to confer a full malignant phenotype on human bronchial epithelial cells. Cancer Res. 2006; 66(4):2116–2128. https://doi.org/10.1158/0008-5472.CAN-05-2521 PMID: 16489012

64. Gaillard H, Garcia-Muse T, Aguilera A. Replication stress and cancer. Nat Rev Cancer. 2015; 15(5):276–289. https://doi.org/10.1038/nrc3916 PMID: 25907220

65. Ait Saada A, Lambert SAE, Carr AM. Preserving replication fork integrity and competence via the homologous recombination pathway. DNA Repair (Amst). 2018; 71:135–147. https://doi.org/10.1016/j.dnarep.2018.08.017 PMID: 30220600

66. Maccaroni K, Balzano E, Mirimao F, Giunta SA-O, Pelliccia FA-O. Impaired Replication Timing Promotes Tissue-Specific Expression of Common Fragile Sites. LID—10.3390/genes11030326 LID—326. Genes (Basel). 2020; 11(3):326–350. https://doi.org/10.3390/genes11030326 PMID: 32204553

67. Chan KL, Palmai-Pallag T, Ying S, Hickson ID. Replication stress induces sister-chromatid bridging at fragile site loci in mitosis. Nat Cell Biol. 2009; 11(6):753–760. https://doi.org/10.1038/ncb1882 PMID: 19465922

68. Durkin SG, Glover TW. Chromosome fragile sites. Annu Rev Genet. 2007; 41:169–192. https://doi.org/10.1146/annurev.genet.41.042007.165900 PMID: 17608616

69. Nickoloff JA. Paths from DNA damage and signaling to genome rearrangements via homologous recombination. Mutation Research. 2017; 806:64–74. https://doi.org/10.1016/j.mrfmmm.2017.07.008 PMID: 28779875

70. Gelot C, Magdalou I, Lopez BS. Replication stress in Mammalian cells and its consequences for mitosis. Genes (Basel). 2015; 6(2):267–298. https://doi.org/10.3390/genes6020267 PMID: 26010955

71. Wilhelm T, Ragu S, Magdalou I, Machon C, Dardillac E, Techer H, et al. Slow Replication Fork Velocity of Homologous Recombination-Defective Cells Results from Endogenous Oxidative Stress. PLoS Genet. 2016; 12(5):e1006007. https://doi.org/10.1371/journal.pgen.1006007 PMID: 27135742

72. Somyajit K, Gupta R, Sedlackova H, Neelsen KJ, Ochs F, Rask MB, et al. Redox-sensitive alteration of replisome architecture safeguards genome integrity. Science. 2017; 358(6364):797–802. https://doi.org/10.1126/science.aao3172 PMID: 29123070

73. Carter SL, Eklund AC, Kohane IS, Harris LN, Szallasi Z. A signature of chromosomal instability inferred from gene expression profiles predicts clinical outcome in multiple human cancers. Nat Genet. 2006; 38 (9):1043–1048. https://doi.org/10.1038/ng1861 PMID: 16921376

74. Barger CJ, Branick C, Chee L, Karpf AR. Pan-Cancer Analyses Reveal Genomic Features of FOXM1 Overexpression in Cancer. Cancers (Basel). 2019; 11(2):251–273. https://doi.org/10.3390/cancers11020251 PMID: 30795624

75. Marechal A, Zou L. DNA damage sensing by the ATM and ATR kinases. Cold Spring Harb Perspect Biol. 2013; 5(9). https://doi.org/10.1101/cshperspect.a012716 PMID: 24003211

76. Nam EA, Cortez D. ATR signalling: more than meeting at the fork. Biochem J. 2011; 436(3):527–536. https://doi.org/10.1042/BJ20102162 PMID: 21615334

77. Wilhelm T, Magdalou I, Barascu A, Techer H, Debatisse M, Lopez BS. Spontaneous slow replication fork progression elicits mitosis alterations in homologous recombination-deficient mammalian cells. Proc Natl Acad Sci U S A. 2014; 111(2):763–768. https://doi.org/10.1073/pnas.1311520111 PMID: 24347643

78. Teh MT, Gemenetzidis E, Chaplin T, Young BD, Philpott MP. Upregulation of FOXM1 induces genomic instability in human epidermal keratinocytes. Mol Cancer. 2010; 9:45. https://doi.org/10.1186/1476-4598-9-45 PMID: 20187950

79. Arlt MF, Wilson TE, Glover TW. Replication stress and mechanisms of CNV formation. Curr Opin Genet Dev. 2012; 22(3):204–210. https://doi.org/10.1016/j.gde.2012.01.009 PMID: 22365495

80. Mazzu YZ, Armenia J, Chakraborty G, Yoshikawa Y, Coggins SA, Nandakumar S, et al. A Novel Mechanism Driving Poor-Prognosis Prostate Cancer: Overexpression of the DNA Repair Gene, Ribonucleotide Reductase Small Subunit M2 (RRM2). Clin Cancer Res. 2019; 25(14):4480–4492. https://doi.org/10.1158/1078-0432.CCR-18-4046 PMID: 30996073

81. Park YY, Jung SY, Jennings NB, Rodriguez-Aguayo C, Peng G, Lee SR, et al. FOXM1 mediates Dox resistance in breast cancer by enhancing DNA repair. Carcinogenesis. 2012; 33(10):1843–1853. https://doi.org/10.1093/carcin/bgs167 PMID: 22581827

82. Bonilla B, Hengel SR, Grundy MK, Bernstein KA. RAD51 Gene Family Structure and Function. LID—10.1146/annurev-genet-021920-092410. Annual Reviews in Genetics. 2020; 54:1–22. https://doi.org/10.1146/annurev-genet-021920-092410 PMID: 32663049

83. Tomimatsu N, Mukherjee B, Catherine Hardebeck M, Ilcheva M, Vanessa Camacho C, Louise Harris J, et al. Phosphorylation of EXO1 by CDKs 1 and 2 regulates DNA end resection and repair pathway choice. Nat Commun. 2014; 5:3561. https://doi.org/10.1038/ncomms4561 PMID: 24705021

84. Wang IC, Zhang Y, Snyder J, Sutherland MJ, Burhans MS, Shannon JM, et al. Increased expression of FoxM1 transcription factor in respiratory epithelium inhibits lung sacculation and causes Clara cell hyperplasia. Dev Biol. 2010; 347(2):301–314. https://doi.org/10.1016/j.ydbio.2010.08.027 PMID: 20816795

85. Kalinina OA, Kalinin SA, Polack EW, Mikaelian I, Panda S, Costa RH, et al. Sustained hepatic expression of FoxM1B in transgenic mice has minimal effects on hepatocellular carcinoma development but increases cell proliferation rates in preneoplastic and early neoplastic lesions. Oncogene. 2003; 22 (40):6266–6276. https://doi.org/10.1038/sj.onc.1206640 PMID: 13679865

86. Kalin TV, Ustiyan V, Kalinichenko VV. Multiple faces of FoxM1 transcription factor: lessons from transgenic mouse models. Cell Cycle. 2011; 10(3):396–405. https://doi.org/10.4161/cc.10.3.14709 PMID: 21270518

87. Wang Z, Park HJ, Carr JR, Chen YJ, Zheng Y, Li J, et al. FoxM1 in tumorigenicity of the neuroblastoma cells and renewal of the neural progenitors. Cancer Res. 2011; 71(12):4292–4302. https://doi.org/10.1158/0008-5472.CAN-10-4087 PMID: 21507930

88. Gu C, Yang Y, Sompallae R, Xu H, Tompkins VS, Holman C, et al. FOXM1 is a therapeutic target for high-risk multiple myeloma. Leukemia. 2016; 30(4):873–882. https://doi.org/10.1038/leu.2015.334 PMID: 26648534

89. Bartkova J, Horejsi Z, Koed K, Kramer A, Tort F, Zieger K, et al. DNA damage response as a candidate anti-cancer barrier in early human tumorigenesis. Nature. 2005; 434(7035):864–870. https://doi.org/10.1038/nature03482 PMID: 15829956

90. Gorgoulis VG, Vassiliou LV, Karakaidos P, Zacharatos P, Kotsinas A, Liloglou T, et al. Activation of the DNA damage checkpoint and genomic instability in human precancerous lesions. Nature. 2005; 434 (7035):907–913. https://doi.org/10.1038/nature03485 PMID: 15829965

91. Bartkova J, Rezaei N, Liontos M, Karakaidos P, Kletsas D, Issaeva N, et al. Oncogene-induced senescence is part of the tumorigenesis barrier imposed by DNA damage checkpoints. Nature. 2006; 444 (7119):633–637. https://doi.org/10.1038/nature05268 PMID: 17136093

92. Molinuevo R, Freije A, de Pedro I, Stoll SW, Elder JT, Gandarillas A. FOXM1 allows human keratinocytes to bypass the oncogene-induced differentiation checkpoint in response to gain of MYC or loss of p53. Oncogene. 2017; 36(7):956–965. https://doi.org/10.1038/onc.2016.262 PMID: 27452522

93. Smirnov A, Panatta E, Lena A, Castiglia D, Di Daniele N, Melino G, et al. FOXM1 regulates proliferation, senescence and oxidative stress in keratinocytes and cancer cells. Aging (Albany NY). 2016; 8 (7):1384–1397.